

Supporting Information

Promoting Active Electronic States in LaFeO₃ Thin-Films Photocathodes via Alkaline-Earth Metal Substitution

Xin Sun, Devendra Tiwari^{†} and David J. Fermin^{*}*

School of Chemistry, University of Bristol, Cantocks Close, Bristol BS8 1 TS, UK

[‡]*Current affiliation: Department of Mathematics, Physics & Electrical Engineering, Northumbria University, Ellison Place, Newcastle upon Tyne NE1 8ST, UK*

*Corresponding authors:

Devendra.Tiwari@northumbria.ac.uk

David.Fermin@bristol.ac.uk

Figure S1. Topography and composition of alkaline-earth metal cation (AMC) substituted LaFeO₃ (LFO).

Figure S2. XRD analysis of AMC substituted LaFeO₃ (LFO).

Figure S3. Deconvolution of La 3d, Fe 2p, O 1s XPS bands of 7% Sr substituted LFO thin-film

Figure S4. Photoelectrochemical responses of AMC substituted LFO in the presence of O₂.

Figure S5. Photoelectrochemical responses of AMC substituted LFO under O₂ free conditions.

Figure S6. Dynamic photocurrent transient responses of pristine and 7% Ba substituted LFO .

Figure S7. Oxygen reduction reaction in the dark as a function of Ba²⁺ content.

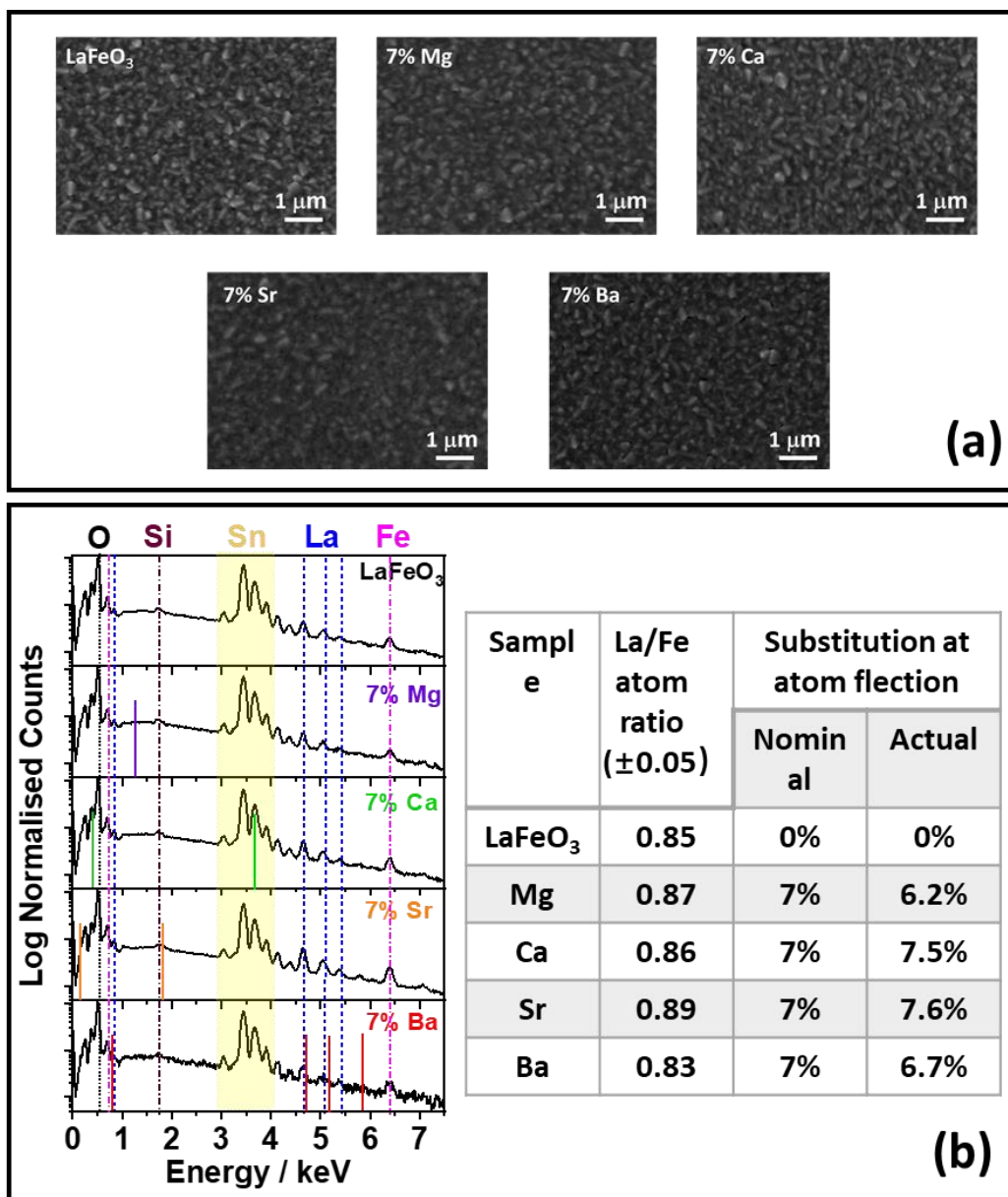


Figure S1. Topography and composition of alkaline-earth metal cation (AMC) substituted LaFeO₃ (LFO): Top view scanning electron micrographs (a) and energy dispersive analysis of X-rays spectra (b) of pristine and 7% AMC substituted LFO thin-films.

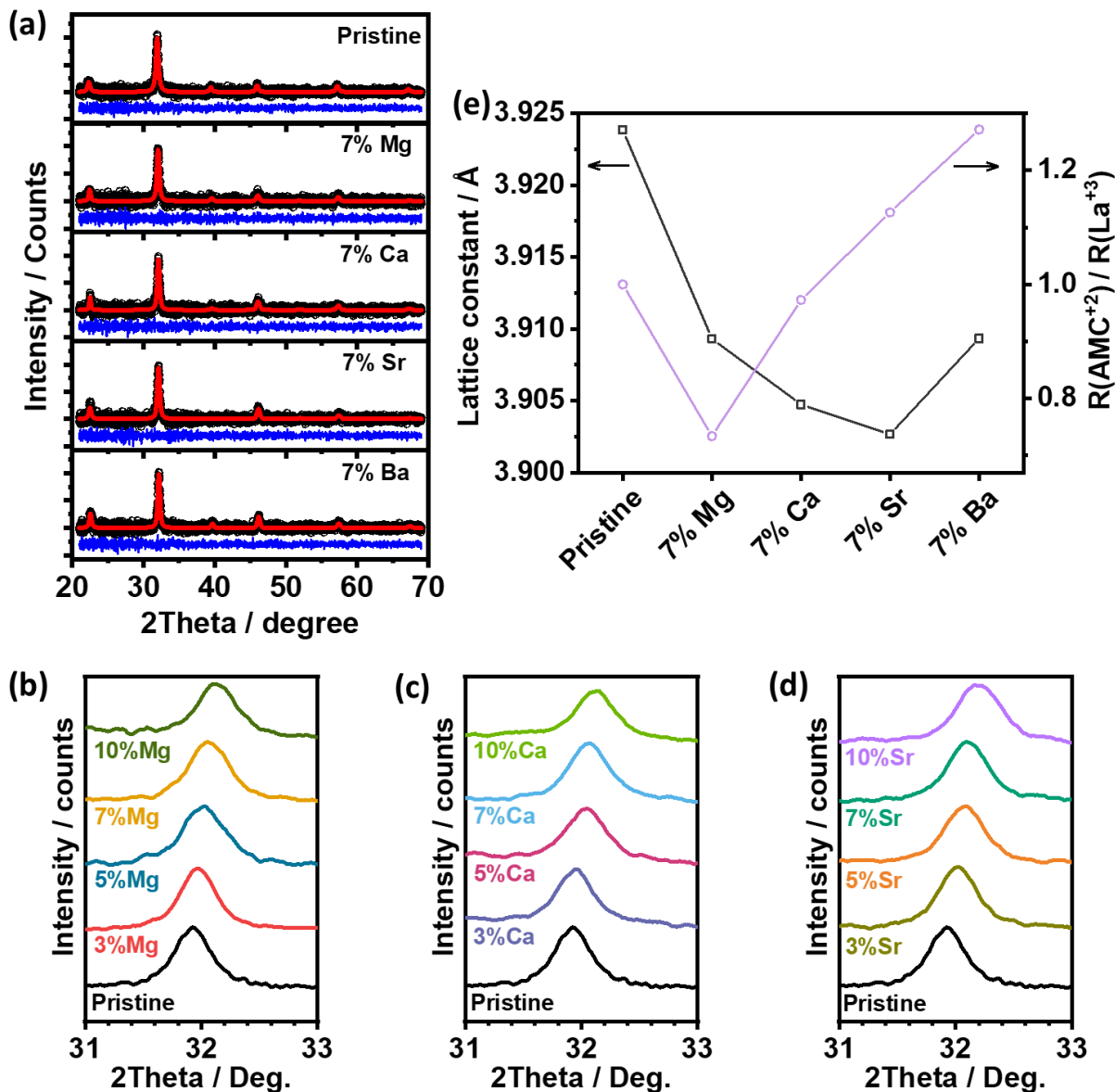


Figure S2. XRD analysis of AMC substituted LaFeO₃ (LFO): (a) XRD patterns of the pristine and 7% AMC substituted LFO refined to the *pm-3m* cubic phase JCPDS-ICDD database file 01-075-0541; evolution of the (110) peak as a function of extent of LFO substitution by (b) Sr²⁺, (c) Ca²⁺ and (d) Mg²⁺. (e) Lattice constant extracted from full-profile structural Pawley refinement shown in (a). Despite the flat difference curve, the refinement could not converge below R_p and R_{wp} of 18% and 23%, respectively. The uncertainty in the refinement arises from the scatter in the experimental XRD and nanoscale crystalline domain of the thin-films. Although the trend is clear and unambiguous, the absolute values of the estimated lattice parameters must be considered cautiously.

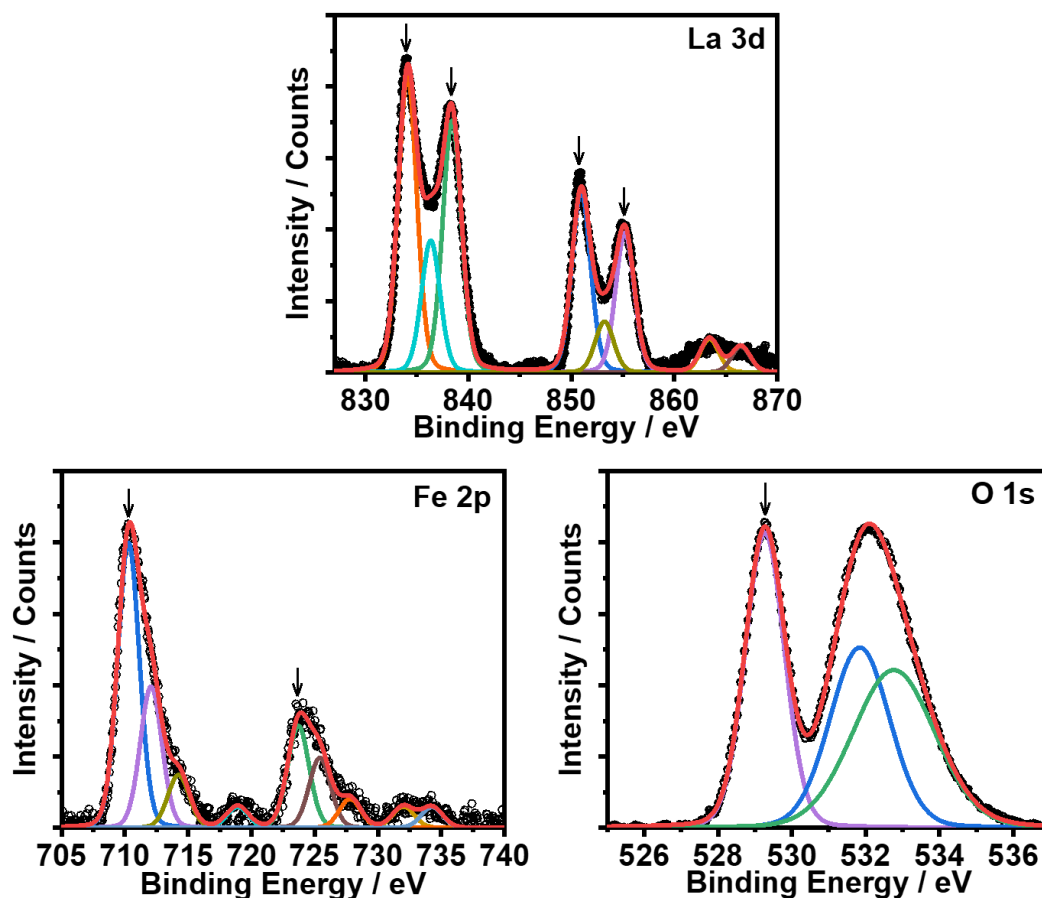


Figure S3. Deconvolution of La 3d, Fe 2p, O 1s XPS bands of 7% Sr substituted LFO thin-film. The La 3d shows two photoemission peaks at 833.9 (La 3d_{5/2}) and 850.9 eV (La 3d_{3/2}) with a 17eV spin-orbit component between the doublet, confirming the La³⁺ oxidation state. The Fe 2p spectrum shows the Fe 2p_{3/2} around 710 eV and Fe 2p_{1/2} at 724.0 eV, with a satellite peak at 724.2 eV. The Fe 2p peak is deconvoluted into three components, with the most prominent associated with Fe³⁺ species and the other two peaks at higher binding energies (BE) correspond to higher iron oxidation states. The O 1s peak shows a sharp band around 529 eV linked to the oxygen in the perovskite lattice, while the other two contributions are assigned to a hydroxyl group and carbonated species. The discussion in the main text focused on the evolution of the Fe 2p_{3/2} and O 1s bands as a function of AMC substitution. However, we also noticed that the higher BE components of the O 1s appear to be affected by AMC substitution (see **Figure 2b** and **2d** of the main text). We rationalise this observation as variations in the relative intensity of the hydroxyl and carbonated photo-emission responses, as opposed to shifts in the binding energy.

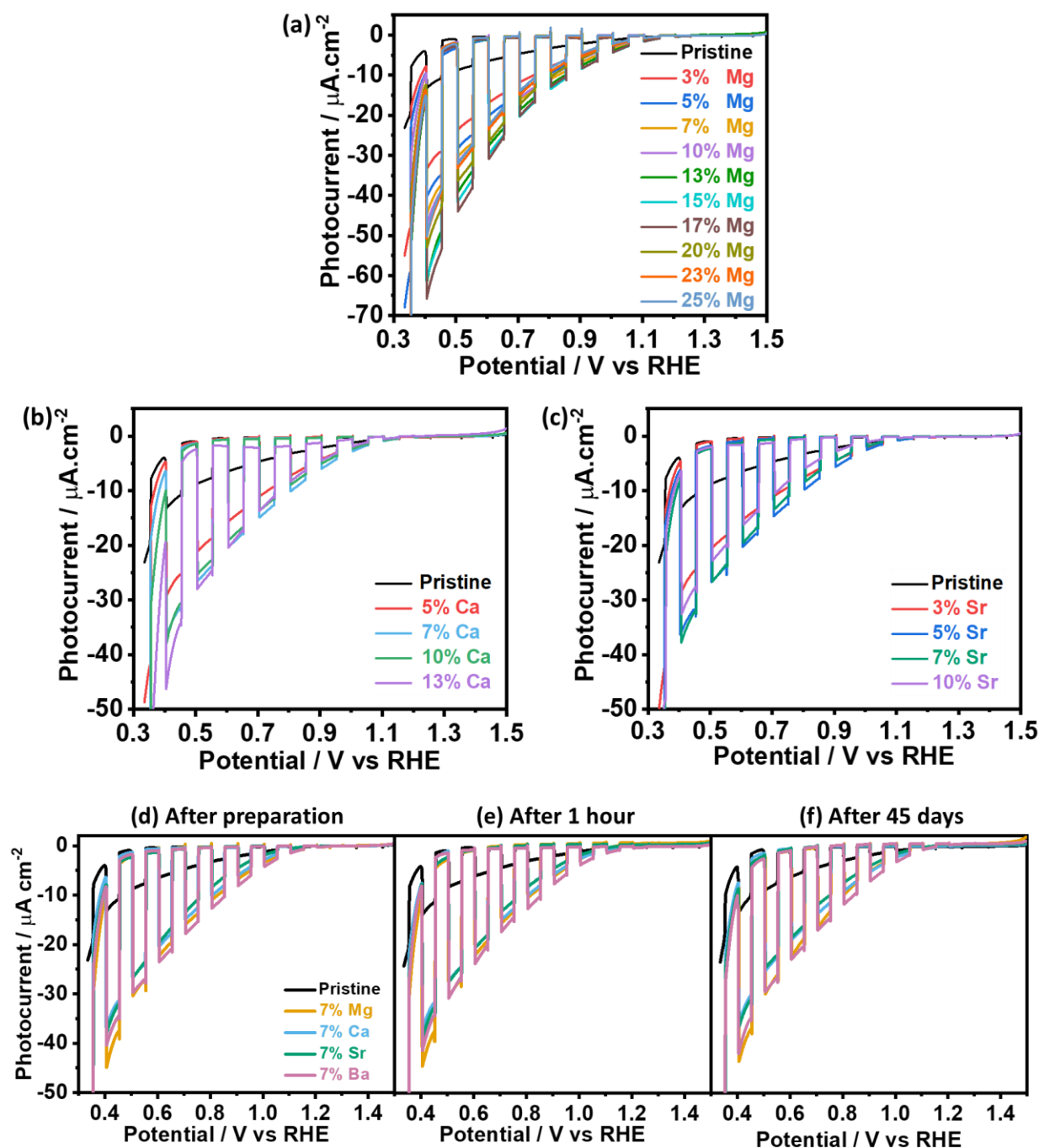


Figure S4. Photoelectrochemical responses of AMC substituted LFO in the presence of O_2 : Linear sweep voltammograms (LSV) of (a) Mg^{2+} , (b) Sr^{2+} and (c) Ca^{2+} substituted $LaFeO_3$ thin-films recorded at 5 mV/s under a square wave 405 nm illumination and photon flux of $3.25 \times 10^{15} cm^{-2} s^{-1}$. LSV curves of the pristine and 7% AMC substituted films recorded under identical conditions: (d) after preparation, (e) after 1 hr of continuous illumination and (f) after 45 days exposed to air. All experiments are recorded under O_2 -saturated aqueous solution containing 0.1 M Na_2SO_4 at pH 12.

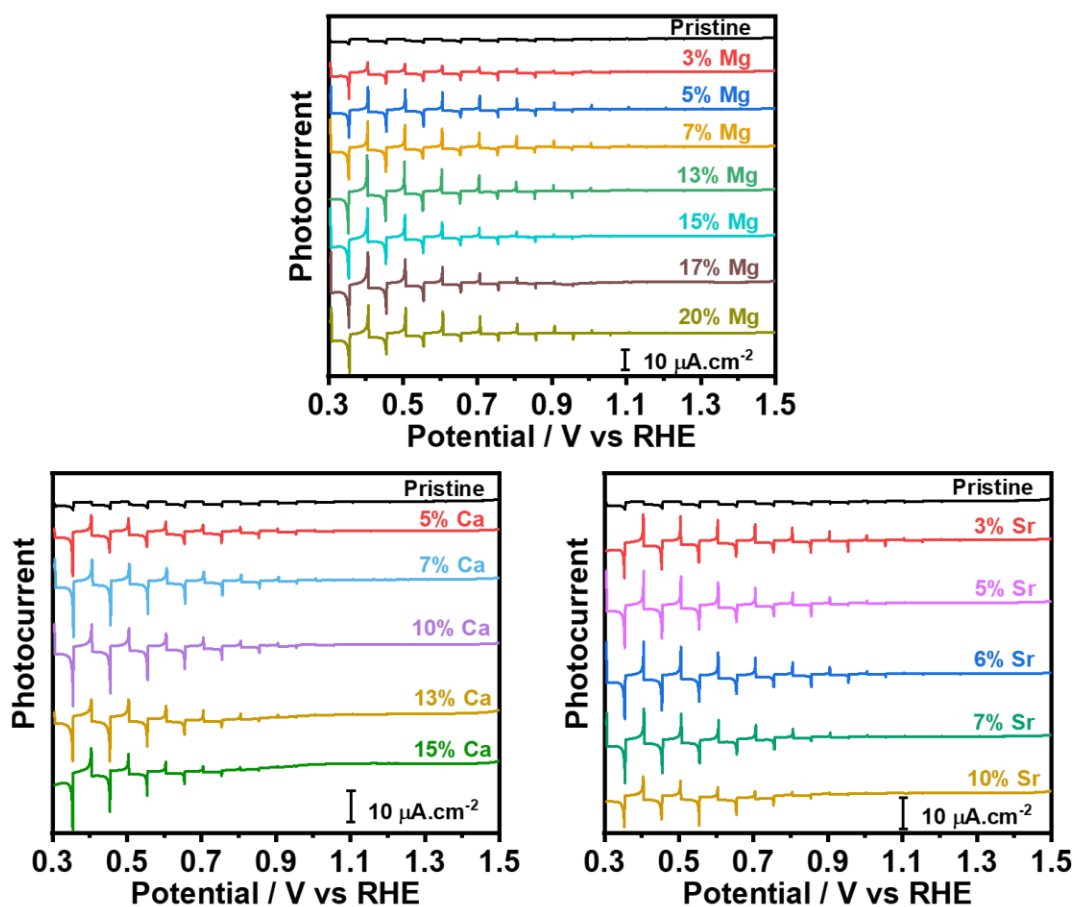


Figure S5. Photoelectrochemical responses of AMC substituted LFO under O_2 free conditions. LSVs (5 mV/s) of LFO films with different substitution levels of Mg^{2+} , Ca^{2+} and Sr^{2+} performed under 405 nm square wave light perturbation (photon flux of $3.25 \times 10^{15} \text{ cm}^{-2} \text{ s}^{-1}$) in Ar-saturated 0.1M Na_2SO_4 aqueous solution pH 12.

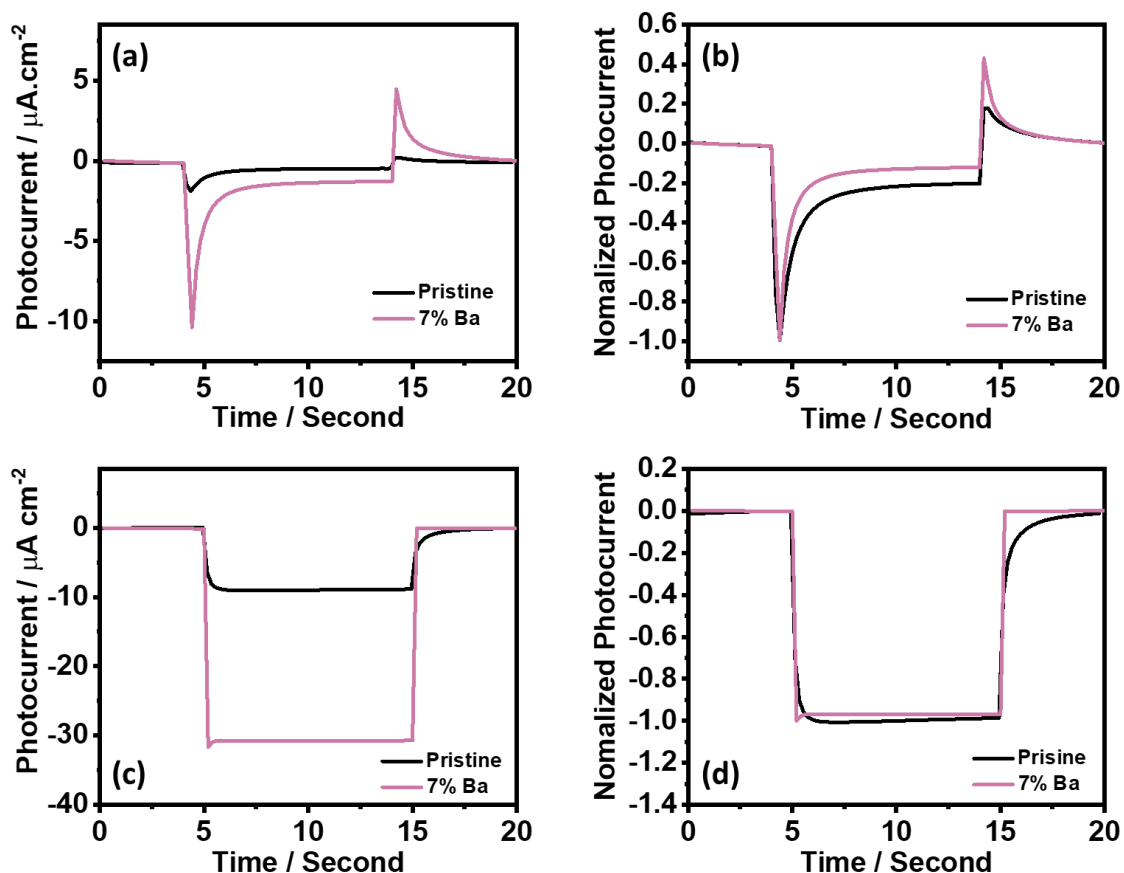


Figure S6. Dynamic photocurrent transient responses of pristine and 7% Ba substituted LFO. Transient photocurrent responses of pristine and 7% Ba^{2+} substituted LFO thin-films at 0.45 V vs RHE in Ar-saturated (a) and O_2 -saturated (c) 0.1M Na_2SO_4 aqueous solution (pH 12). The films are illuminated with a 405 nm LED ($3.25 \times 10^{15} \text{ cm}^{-2} \text{ s}^{-1}$ photon flux). (b) displays photocurrent transients normalised by the maximum photocurrent under Ar-saturated solution, showing a comparatively smaller photostationary current at 7% Ba^{2+} substituted films. (d) shows normalised photocurrent responses in O_2 saturated solutions. The figure shows that AMC substitution not only increases the overall photocurrent (c) but also decreases the response time during the on and off-transients. This is linked to the dampening of the A-states responsible for majority carrier trapping upon AMC substitution.

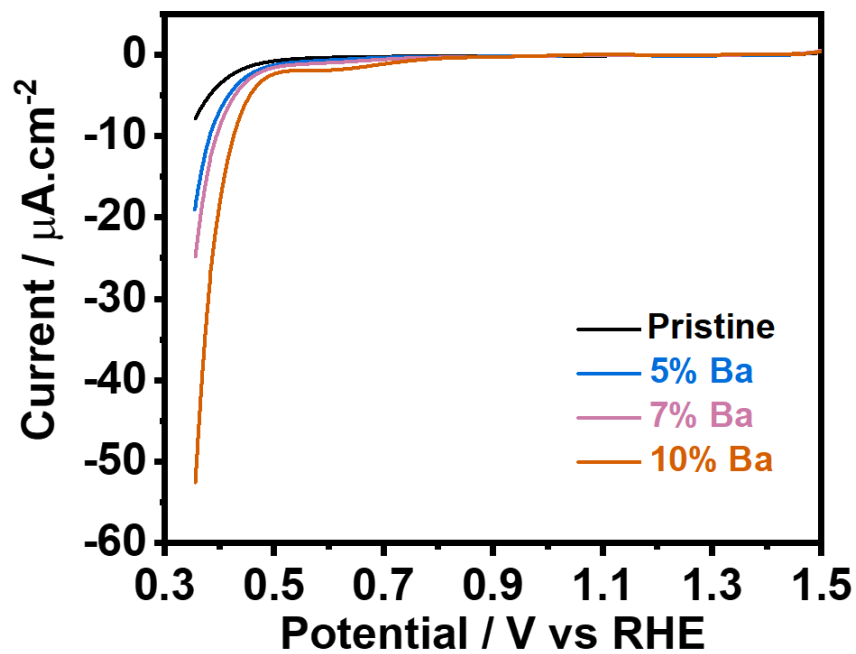


Figure S7. Oxygen reduction reaction in the dark as a function of Ba^{2+} content. Electrochemical responses Linear-sweep voltammograms recorded at 5 mV/s for pristine and Ba substituted LaFeO_3 in O_2 -saturated Na_2SO_4 aqueous solutions (pH 12) in the dark.